WORLD CONFERENCE ON TIMBER ENGINEERING 2025
BRISBANE, AUSTRALIA
Advancing Timber for the Future Built Environment

VERTICAL AND SHEARING PERFORMANCE OF KUMIMONO USED IN TRADITIONAL WOODEN STRUCTURES

Iuko Tsuwa [1], Mikio Koshihara [2]

ABSTRACT: This study focused on the structural performance of *Kumimono* for structural analysis of traditional wooden architecture such as five storied pagodas, temples amd shrines. *Kumimono* is called bracket complexes in English, and is a component between columns and a roof. In a previous research, it is said that vertical perfrmance of *Kumimono* has an influence of the vertical motion of a whole building. However the vertical stiffness of *Kumimono* is not clear quantitatively. Therefore we conducted compression tests for one *Kumimono* at first. In the tests, we had some various test cases changing how to apply vertical load because the parts in actural traditional buildings have a possibility to have some gap due to deterioration over time and vertical load way can change. Furthermore, horizontal loading tests applying moment and shearing force for two *Kumimono* was conducted. We verified the evaluation method for the compression performance and shearing performance applying vertical load based on those experimental results.

KEYWORDS: Bracket complexes, Compression stiffness, Shear stiffness, Traditional timber structure, Seismic performance

1 – INTRODUCTION

In this study, we conducted experimental tests foucusing on vertical structural performance of *Kumimono*, called bracket complexes in English, used in traditional wooden architecture such as five storied pagodas, temples and shrines. We verified the evaluation method for the compression performance and shearing performance applying vertical load based on the results of two types of experiments.

Prof. Kawai et al. studied the effect of the bending deformation of a whole building on the vibration characteristics of a pagoda in a previous research [1]. They claimed that vertical deforrmation at *Kumimono* and a roof affected on the vertical motion of each floor. However the vertical performance of *Kumimono* is not clear. In addition, seismic performance of *Kumimono* of including within a whole structure and combining with other seismic elements are not clarified. Thus we conducted compression tests of one *Kumimono* and grasped vertical stiffness quantitatively. Furthermore, we carried out static horizontal loading tests by applying moment and shear force with two *Kumimono*. The test results were compared with the compression test results of one *Kumimono.* In addition, the evaluation method for the vertical stiffness and shear stiffness of *Kumimono* was verified based on vertical stiffness from our experimental results and the existing evaluation method for the shear stiffness.

2 –EXPERIMENT FOR ONE UNIT OF KUMIMONO

2.1 EXPERIMNETAL METHOD

A compression test was conducted on one *Asuka*-style *Kumimono* using the method shown in Fig.1. Eight patterns of loading were performed by changing the pattern of vertical load on the *Kumimono* and assuming the positions of the support points as shown in Fig.2. The reason for assuming different support points is that, when looking at actual shrine and temple architecture, it is thought that in buildings that have been used for many years, gaps may form between components due to deterioration over time, which may change the way the vertical load is applied to the *Kumimono*. We will understand from several vertical load patterns how the uneven load application to each of bearing blocks and bracket arms that make up the *Kumimono* affects the

[1] Iuko Tsuwa, Structural desing division, The Japanese Association for Conservation of Architectural Monuments, Tokyo, Japan, tsuwaiuko@gmail.com

[2] Mikio Koshihara, Institute of Industrial Science, The University of Tokyo, Tokyo, Japan, kos@iis.u-tokyo.ac.jp

https://doi.org/10.52202/080513-0667

compression performance of the *Kumimono* and the flow of force within *Kumimono*.

2.2 TEST SPECIMEN

The size of the test specimen was set to the equivalent of a column diameter of 300mm. The elevation of the test specimen is shown in Fig.3.

2.3 EXPERIMNETAL RESULTS

Fig.4 shows the relationship between the load and the displacement measured at a large bearing block (*Daito*) as the displacement of the whole test specimen. The load-displacement relationship showed that all test specimens had slight sliding deformation from the initial state. C3 and C5, which had few support points, and C6, which had an asymmetrical support point arrangement, tended to have lower stiffness than the other cases.

The load distribution of each load cell obtained in the experiment is shown Fig.5. As a result of placing load cells at each part of the layer between bracket arms and cloud bearing blocks, the ratio of stress on the cloud bearing block layer was as follows.

Cloud bearing block (left): Center: Cloud bearing block (right): Small bearing block: Cloud bracket arm ≒ 1 : 3 : 1 : 1 : 0.5

When there was a support point only in the center or when the bracket was in a balance state, the load tended to flow to the part with the support point, but the difference in the load was not very large, and the ratio was similar for all loading cases.

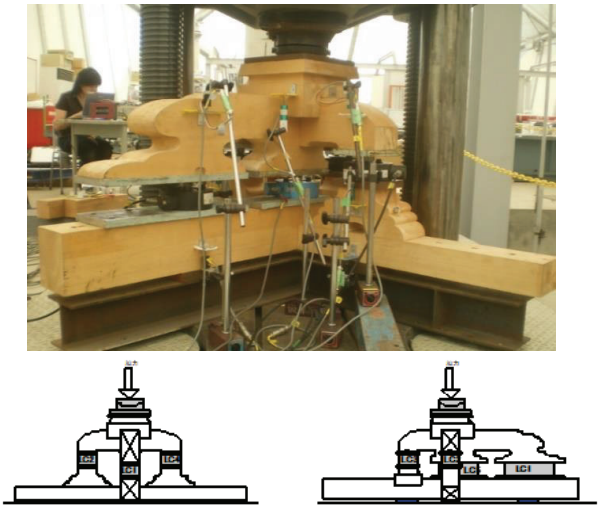

Figure 1. Compression test method

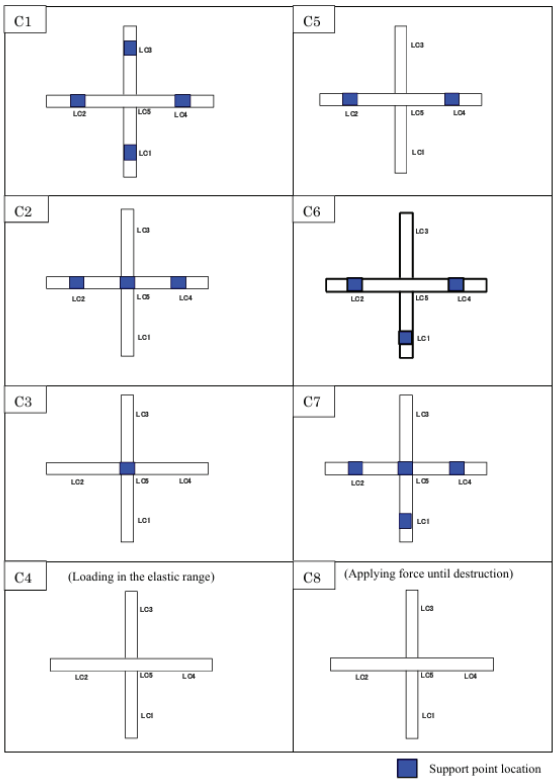

Figure 2. Loading case

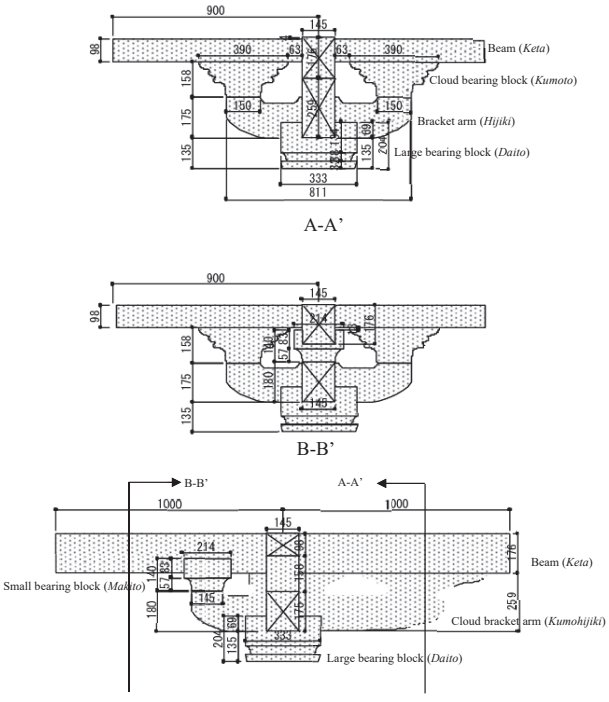

Figure 3. Test specimen dimensions

https://doi.org/10.52202/080513-0667

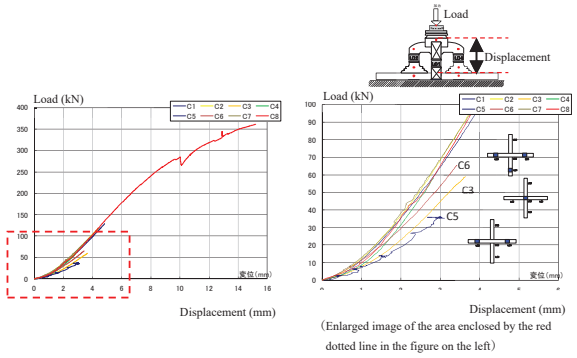

Figure 4. Load and displacement relationship

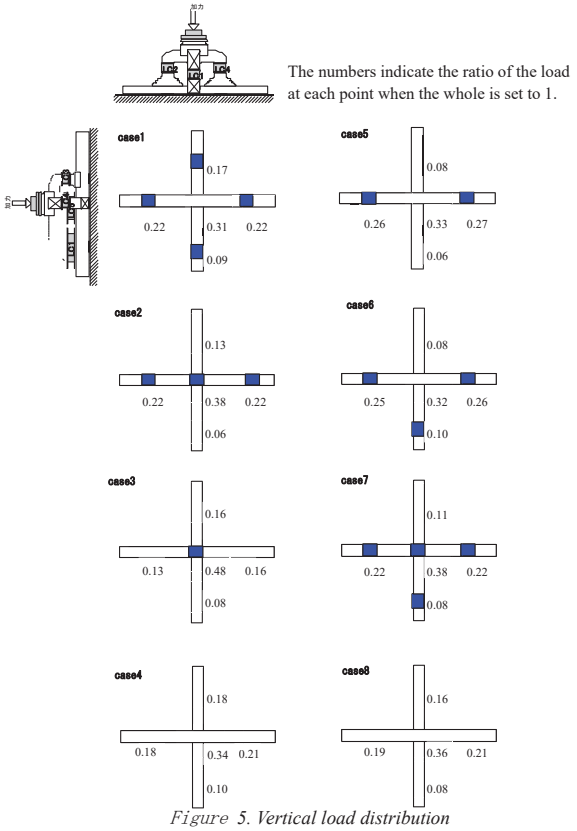

Figure 5. Vertical load distribution

3 – EXPERIMENT FOR TWO UNITS OF KUMIMONO

3.1 EXPERIMNETAL METHOD

As mentioned in Chapter 1, we assumed that each story of the five-story pagoda was subjected to moment and shear force, and performed static loading experiments in which bending and shear were simultaneously applied to two *Kumimono*, and calculated the vertical and shear stiffness of each *Kumimono*.

Two *Kumimono*, which were assumed to be the first floor of an Asuka-style five-story pagoda, were installed on a steel frame as shown in Fig.6, and a static horizontal load experiment was conducted by repeatedly loading the two *Kumimono* with positive and negative forces three times each. A moment and shear force were applied to two *Kumimono* by applying a horizontal force to the steel frame fastened to them. In addition, by changing the height of the load point, static loading experiments were carried out assuming several ratios of moment and shear force applied to the structure.

The test specimens for this experiment were also of the same dimensions as the specimen in the previous chapter. The size was set to the equivalent of a column diameter of 300mm, which was the same size as the first story of an *Asuka* style five-story pagoda, scaled down by 2/3. The material used was Japanese cypress.

The vertical load of the test specimen was calculated from the weight of one pillar of a five-story *Asuka*-style pagoda, and was set so that the stress intensity would be constant when the specimen was 2/3 its original size. The weight of the steel frame and the tensile force of the jack were combined to apply a load of 107.8kN (11 tonf) per pillar.

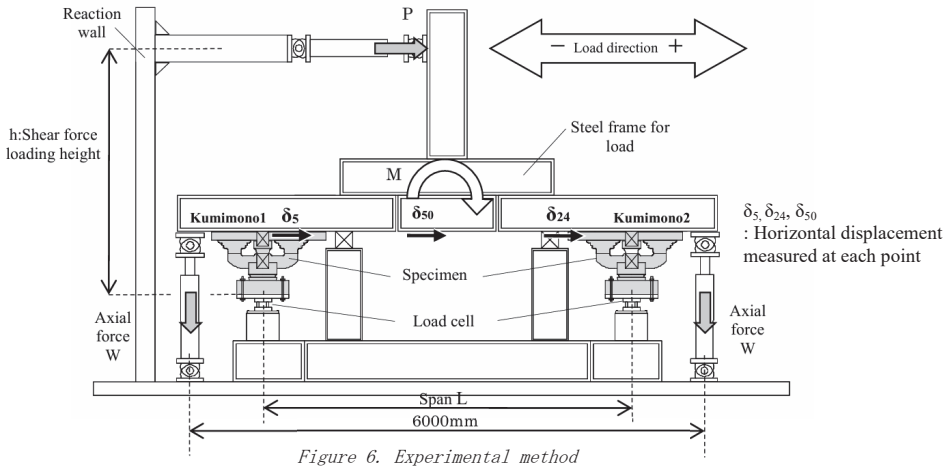

Figure 6. Experimental method

https://doi.org/10.52202/080513-0667

3.2 EXPERIMENTAL CASE

Four loading cases were set with the height of the load point as a parameter as shown in Table 1. Case 1 had a low load point and shear force was predominant, Cases 2 and 3 had gradually higher load points and increased moment compared to Case 1, and Case 4 had bending force predominating. Although the width between two *Kumimono* was assumed to be 4.3m and the height approximately 10m in Case 4, the width-to-height ratio was changed to 1.80m wide and 4.705m high and loading was performed assuming a load point height of approximately 10m because it was not possible to apply force at the 10m position due to the limitation of the test site.

The force was controlled at the deformation angles shown in Fig.7. The target deformation angles were 1/500, 1/250, 1/200, and 1/120 rad., and the force was repeatedly applied three times for each as shown in Fig.8.

3.3 EXPERIMNETAL RESULTS

Fig.9 shows a graph overlaying the horizontal load-horizontal displacement relationships for Cases 1 to 4. The horizontal displacement was the largest in Case 1 because the shear force was predominant, and as the applied moment increased, the displacement occured with a smaller load.

Fig.10 shows graphs on M-δ_θ and Q-δ_Q from the data of δ_5. The measured horizontal displacement was decomposed into rotational and shear deformations. In the M-δ_θ graph, positive and negative asymmetry was observed in the hysteresis loop in Cases 3 and 4. In addition, the deformation angle increased from Cases 2 to 4. In the Q-δ_Q graph, it became clear that the maximum shear displacement at the girder level decreased as the applied moment increased. Furthermore, the slippage of displacement seen after unloading in Cases 1 and 2 was not observed in Cases 3 and 4.

Fig.11 shows the proportion of rotational deformation. The left side of Fig.11 shows each case and the right one shows each derformation step of Case 4. Ch5 and Ch24 show the rotational deformation of each Kumimono obtained from δ_5 and δ_{24}, and Ch50 shows the rotational deformation of the whole *Kumimono* δ_{50} as shown in Fig.6. In Cases 1 to 3, the proportion of rotational deformation was less than 10%, and it can be said that the displacement of *Kumimono* is dominated by displacement due to shear.

Fig.12 shows deformation diagrams drawn from the horizontal displacement of each component of Kumimono. In Case 1, the deformation diagram is almost symmetrical, whereas in Case 4, it showed an asymmetric shape. In Case 4, the behavior of bracket arms (*Hijiki*) and a large bearing block (*Daito*) at δ5 and a large bearing block at δ24 were characteristic, and it is believed that the whole *Kumimono* rotated around the large bearing block during hehaviour.

Table 1: Loading case

Case	Axial force W (tonf)	Width L (m)	Loading Height h (m)	Remarks
Case1	22 (11+11)	4.3	1.205	Constant axial force, Shear force is predominat
Case1	22 (11+11)	4.3	2.955	Constant axial force, Add moment to case1
Case1	22 (11+11)	4.3	4.705	Constant axial force, Add moment to case2
Case1	22 (11+11)	1.8	4.705	Constant axial force, Moment is predominat

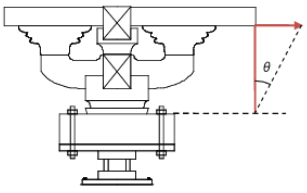

Figure 7. Deformation angle

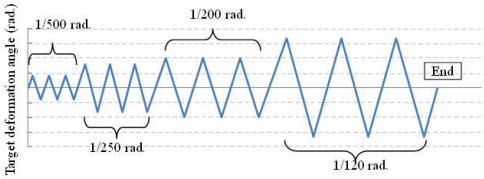

Figure 8. Loading plan

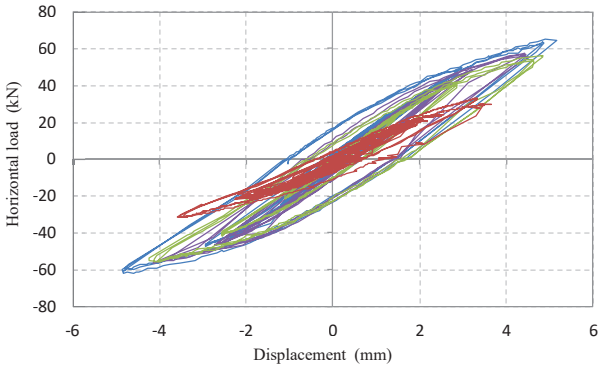

Figure 9. The relationship between horizontal load and displacement from one Kumimono

https://doi.org/10.52202/080513-0667

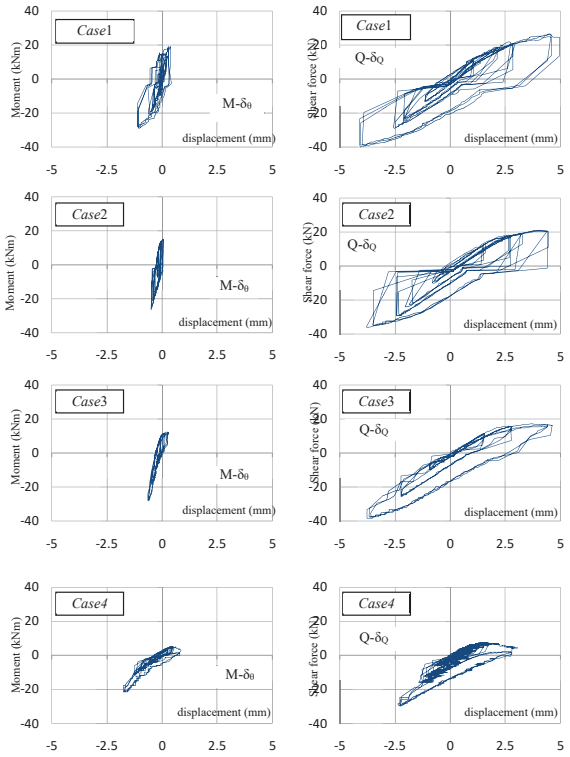

Figure 10. M-δ_θ and Q-δ_Q relataionship

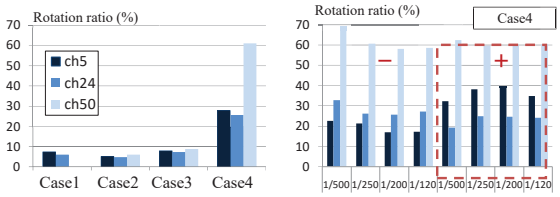

Figure 11. Rotational deformation ratio (Left side: Average rotational deformation ratio at 1/120rad., Right side: the result of Case4)

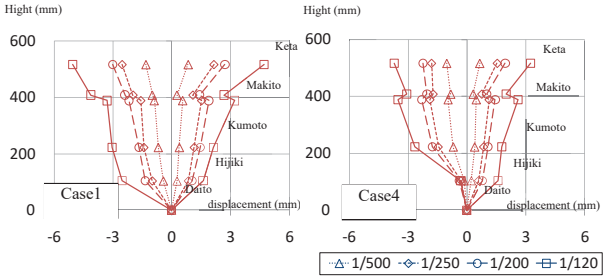

Figure 12. Test specimen deformation diagram

4 – DISCUSSION

4.1 SHEAR STIFFNESS

The shear rigidity of one *Kumimono* was verified based on the experimental results of two units.

The experimental envelope curves of the shear force-shear displacement relationship for each loading case are shown in Fig.13. Kumimono1 is *Kumimono* on the left in Fig.6, and Kumimono2 is *Kumimono* on the right in Fig.6. In all loading cases, the histories of the left and right *Kumimono* were different, and it was confirmed that the shapes were not symmetrical about the origin.

Table 2 shows the results of calculating the tangential stiffness at ±0.001 rad. with Fig.13 as the initial stiffness of the shear spring. The stiffness decreased as the proportion of the moment applied to the *Kumimono* layer increased in case 4. The theoretical value of this initial stiffness was obtained using a previous evaluation method [2]. The experimental value in this small area was 0.94 to 1.05 times the theoretical value, which was relatively consistent.

4.2 EFFECT OF AXIAL FORCE

According to a previous research [2], when static friction changes to kinetic friction, shear stiffness transitions from the first stiffness to the second stiffness. The frictional force caused by the axial force was related to shear stiffness, and when the axial force changed, the frictional force and shear stiffness changed. In other words, it is thought that changes in axial force affected the frictional force and shear stiffness. For example, when a moment was applied to a *Kumimono* layer, if the applied axial force becomes larger in one *Kumimono* and the frictional force became larger, the shear stiffness of the *Kumimono* increased. It is thought that the applied axial force became smaller in the other *Kumimono*, the frictional force became smaller, and the shear stiffness also became smaller. The behaviour image is shown in Fig.14.

Therefore, in order to confirm the effect of axial force fluctuation, the friction force (axial force × μ) - shear displacement relationship obtained by multiplying the axial force of each *Kumimono* obtained in the experiment by the friction coefficient μ was superimposed on the shear force - shear displacement relationship in Fig.13. Here, case 2 is shown in Fig.15. The value of the friction coefficient μ was set to 0.2 here. Kumimono1 rised due to the decrease in axial force, and the shear stiffness appeared to decrease from point A on the figure onwards.

On the other hand, the increase in axial force created sufficient friction, so the shear stiffness was thought to not decrease in Kumimono2,. The effect of axial force fluctuations on the shear stiffness of *Kumimono* can be seen.

https://doi.org/10.52202/080513-0667

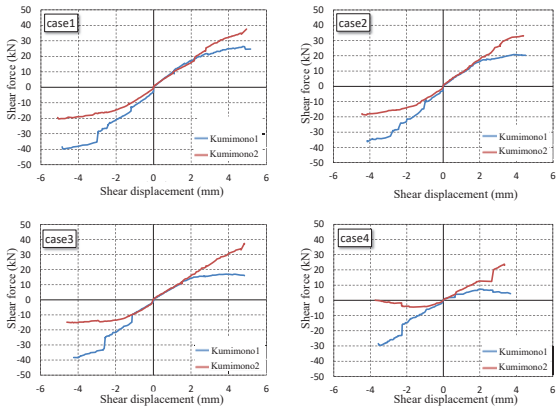

Figure 13. The envelope curves of the shear force-shear displacement relationship

Table 2: Shear stiffness

	Case1	Case2	Case3	Case4
Experiment value	8.0	7.3	7.0	4.9
Theory value	8.3	7.8	6.7	4.7

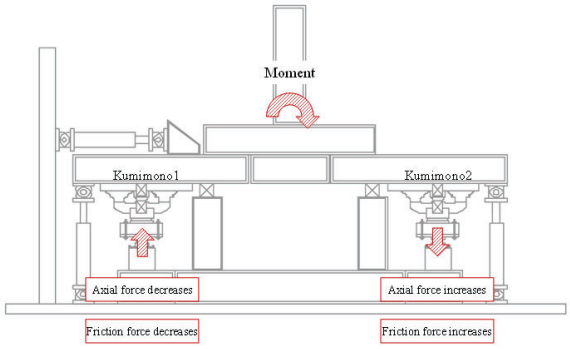

Figure 14. Effect of axial force

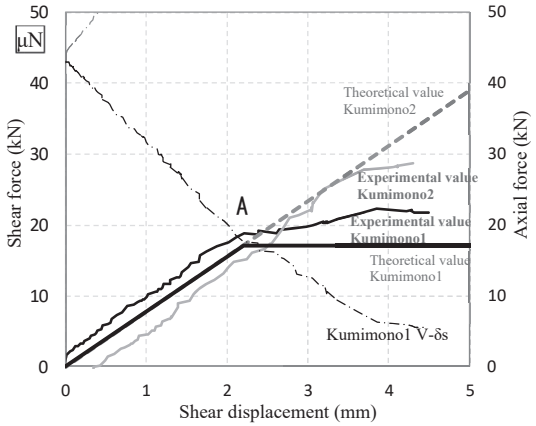

Figure 15. Relationship between axial force, friction force and shear force

4.3 VERTICAL STIFFNESS

As shown in Table 3, the slope of the envelope drawn from the axial force-vertical displacement relationship was used as the vertical stiffness, and the value was calculated from a linear approximation. Except for Case 1, where shear force was dominant, the values were distributed between 50 and 65 kN/mm, with an average of 56 kN/mm. This shows that the vertical stiffness was constant within the elastic range.

Next, we compared the results of two *Kumimon* with the compression test results of one *Kumimono*. Fig.16 shows the envelope curve obtained from the relationship between the axial load and vertical displacement, and the envelope curve obtained from Case 3 in the two-unit experiment. A value of 35.5 kN/mm was obtained for the vertical stiffness of *Kumimono* alone. Compared to the vertical stiffness values obtained in the two-unit experiments, Cases 2 to 4, the vertical stiffness of the two-unit experiment was approximately 1.4 to 1.8 times higher.

4.4 INFLUENCE OF SHEAR SPRINGS AND VERTICAL SPRINGS

In order to model the *Kumimono* layer using shear springs and vertical springs, we examined the relationship between shear springs and vertical springs. We also compared the results with previous experimental results in a previous research [3] using a 1/5 scale model of a five-story pagoda. In order to clarify the behavior of the *Kumimono* layer when shear force and moment were applied to two *Kumimono* units, we verified the relationship between the ratio of horizontal force and moment applied to the *Kumimono* layer and the ratio of displacement due to rotational behavior in horizontal displacement.

Table 4 shows shear force and moment ratio in each case. Fig.17 and Fig.18 show M/Q (moment/shear force applied to *Kumimono*) - δm/δh (rotational deformation/horizontal deformation) relationship from each case and *Kumimono*. The ratio of rotational deformation was minimal at less than 3% until the ratio of shear force and moment applied to *Kumimono* (Q:M) was around 1:15. Even at around 1:20, where the moment was dominant, the result was around 8%. Since this experiment was conducted in the elastic range, it can be said that shear deformation was dominant in the deformation of *Kumimono* in the elastic range.

https://doi.org/10.52202/080513-0667

Table 3: Vertical stiffness (kN/m)

	Case1	Case2	Case3	Case4
Kumimono 1	-13.0	56.1	54.6	50.2
Kumimono 2	27.5	64.2	60.8	49.3

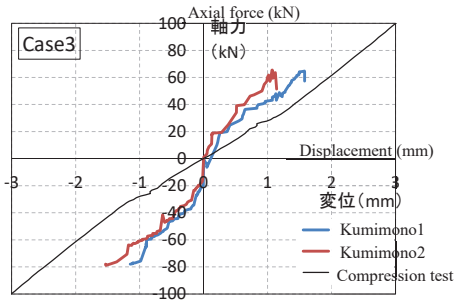

Figure 16. Comparison of two-unit experiment and single unit compression test

Table 4: Shear Force and Moment Ratio

Case	Case1	Case2	Case3	Case4
Q : M	1 : 1	1 : 4.72	1 : 8.43	1 : 20.14

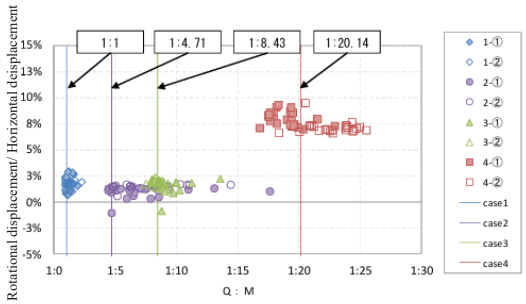

Figure 17. Q:M and δ_θ/δ_Q relataionship for each case

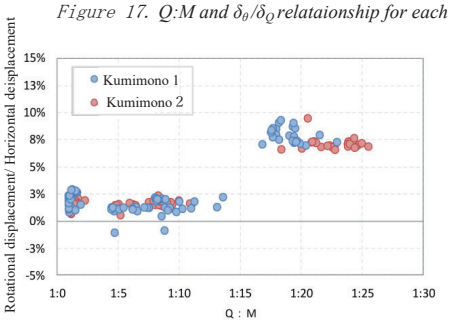

Figure 18. Q:M and δ_θ/δ_Q relataionship for each kumimono

5 – CONCLUSION

Vertical performance of *Kumimono* was determined through compression tests on one *Kumimono*. Additionally, static loading tests were conducted on two *Kumimono*, simultaneously applying shear force and moment, and the shear and vertical performance was examined in particular in the *Kumimono* layer of the five-story pagoda. As a result, the following became clear:

- When a moment was applied to the *Kumimono* layer, the axial force applied to one *Kumimono* fluctuated due to rocking of the layer, which changed the frictional force and the shear stiffness. It clarified the effect of axial force fluctuations on the shear stiffness of the *Kumimono*.

- Vertical stiffness was constant within the elastic range.

-Shear deformation dominated *Kumimono* whole deformation compared to deformation due to rotational behavior within the elastic range, and vertical stiffness is approximately 8 to 10 times the shear stiffness.

6 – REFERENCES

[1] N. Kawai et al.: Research on Dynamic Characteristics of Five-story Pagodas. The report of Grants-in-Aid for Scientific Research between 2004-2006, 2007

[2] Fujita, K., et al., Hysteresis model and stiffness evaluation of bracket complexes used in traditional timber structures based on static lateral loading tests, Journal of structural and construction engineering, No.543, pp.121-127, 2001

[3] K. Chiba et al.: Seismic Performance of Five Storied Pagoda Based on Scaled Model Experiment Part 1-8. Summaries of Technical Papers of Annual Meeting Architectural Institute of Japan, C-1, 481 482, 2005.9

https://doi.org/10.52202/080513-0667